Investigation of nonlinear restoring stiffness in dynamic analysis of tension leg platforms

I. Senjanović *, M. Tomić, S. Rudan

[a] University of Zagreb, Faculty of Mechanical Engineering and Naval Architecture, I. Lučića 5, 10000 Zagreb, Croatia

ABSTRACT

Shortcomings of the traditional stiffness matrix in dynamic analysis of TLPs, derived by considering equilibrium of forces, are pointed out, as well as dilemma concerning consistency of the recently presented matrix based on energy balance. New stiffness matrix is derived by utilizing both force equilibrium approach, with algebraic averaging and root mean square of tendon forces, and energy balance approach for large surge and sway. Yaw is treated as a small and large displacement. Static numerical analysis is performed for all six cases by imposing surge force and yaw moment. The obtained results are compared with those of FEM analysis, and useful conclusion is drawn, which can be used for improvement of uncoupled mathematical model of TLPs.

© 2013 Elsevier Ltd. All rights reserved.

1. Introduction

Tension leg platform (TLP) is classified as a compliant offshore structure, i.e. a semi-submersible one attached to the sea bottom by vertical pretensioned tendons or tethers, [1]. It is ordinary used for deep water oil operations. At the beginning the installed depth was 147 m, *Hutton* (1984), and nowadays it reaches much higher values, for instance 1425 m, *Magnolia* (2005). The consisting parts of a TLP are: pontoon, columns and deck with drilling equipment, [2].

TLP motion in waves is nonlinear due to nonlinear restoring stiffness and damping, [3]. The tendons make TLPs more mobile in horizontal than in vertical plane and ensure almost horizontal position of the working area. Vertical excitation is caused by the first order wave forces, while dominant horizontal excitation is due to the second order wave forces, [4]. Vertical response, i.e. heave, roll and pitch, has high natural frequencies due to high axial tendon stiffness. Natural frequencies of horizontal motion, i.e. surge, sway and yaw, are much lower due to tendon geometric stiffness and can easily fall into resonance with the forcing frequency.

Restoring stiffness plays very important role in TLPs dynamic behavior. Horizontal motion is nonlinear since stiffness is function of surge, sway and yaw. Stiffness of vertical motion is almost linear and depends on platform offset, which causes setdown, as position

parameter. Setdown is one of very important design parameters for limiting platform immersion [5].

Nowadays, the secant stiffness matrix introduced in [6] and slightly modified in [7,8] is still widely used for dynamic analysis of TLPs. Its formulation is based on equilibrium of restoring forces due to large displacements. One finite displacement is imposed while the others are restrained. Asymmetric stiffness matrix for six d.o.f. is established with respect to the center of gravity. Shortcomings of that formulation is that stiffness elements of surge, sway and yaw depend on tendon axial stiffness instead of a buoyancy increase due to setdown, as a hydrostatic spring. The former stiffness is much larger than the latter, and since setdown is not taken into account, implication is excessively large stiffness of horizontal motions. By considering equilibrium due to particular displacements, coupling motions is not taken into account. These problems are analysed in details in [9].

Recently, another formulation of nonlinear restoring stiffness for TLPs is presented in [10], specifying also the shortcomings of the above mentioned traditional one. The stiffness matrix is derived by the energy approach and employing Lagrange's equations. Since the tendon setdowns are different due to coupling of surge and sway with yaw, the platform is considered as independent quadrants, which follow the tendon top motion. Potential energy of the system is established under that assumption, and its first derivatives per displacements give the restoring forces, i.e. secant stiffness matrix. The shortcomings of the traditional stiffness are overcome, i.e. stiffness of horizontal motion depends on platform

---

hydrostatics, and coupling between surge, sway and yaw is captured.

Dynamic analysis of TLP is performed by the uncoupled and fully coupled models [11]. In the former case platform is considered as a rigid body without tendon influence, and linear restoring is applied. If nonlinear damping is linearized problem can be solved in frequency domain. That advantage of reduction of computing time is paid by decreased accuracy.

Fully coupled model is actually 3D FEM model of platform and tendons adapted to large displacements. Due to mechanical and hydrodynamical nonlinearity problem is analysed in time domain. Nonlinear equation of motion can be linearized that makes some difficulties and limitations.

Motivated by the fact that the uncoupled dynamic analysis of TLPs is widely performed by using linear or an inadequate nonlinear restoring stiffness matrix, research for consistent stiffness is undertaken [9]. The force equilibrium approach is employed and stiffness similar to that in [10], determined by the energy approach, is obtained. New stiffness elements are the same for surge, sway and yaw, but without some additional coupling terms present in the energy formulation [10]. Hence, there is doubt which of the two stiffness formulations is a proper one.

In order to overcome that dilemma nonlinear restoring stiffness is derived in this paper by employing both the force equilibrium and energy balance approach for large surge and sway, as well as yaw motion that was not the case in the previous considerations, [9] and [10]. Then, the obtained stiffness expressions are reduced for the case of small yaw.

In order to evaluate two different restoring stiffness formulations, static response of a TLP platform exposed to surge force and yaw moment is analysed, treating yaw both as a small and large quantity. The obtained results are compared to those determined by FEM analysis that leads to some interesting conclusion.

2. Stiffness based on equilibrium of forces

2.1. Large translation and rotation

A double symmetric rectangular TLP, with four tendons and main dimensions shown in Fig. 1, is considered. The platform is exposed to large surge, sway and yaw, δ_x, δ_y and φ, which are common for all tendons, Fig. 2. Trajectory of the tendon top due to yaw is circular arc, $r\varphi$, where r is the tendon radial distance from the platform centroid. The tendon final offset is determined with the secant displacement, Fig. 2

$$\delta_\varphi = 2r \sin \frac{\varphi}{2}. \tag{1}$$

According to Fig. 2 the tendon top coordinates in the local coordinate system read

$$L_x^n = \delta_x - \Delta_x^n = \delta_x - \delta_\varphi \sin \left(\theta_n + \frac{\varphi}{2}\right), \tag{2}$$

$$L_y^n = \delta_y + \Delta_y^n = \delta_y + \delta_\varphi \cos \left(\theta_n + \frac{\varphi}{2}\right), \tag{3}$$

$$L_z^n = \sqrt{L^2 - (L_x^n)^2 - (L_y^n)^2}$$
$$= L \left\{1 - \frac{1}{L^2}\left(\delta_x^2 + \delta_y^2 + \delta_\varphi^2\right) + \frac{2\delta_\varphi}{L^2}\left[\delta_x \sin\left(\theta_n + \frac{\varphi}{2}\right) - \delta_y \cos\left(\theta_n + \frac{\varphi}{2}\right)\right]\right\}^{\frac{1}{2}}, \tag{4}$$

where L is tendon length and θ_n, $n = 1, 2, 3, 4$, is tendon central angle.

Components of the tendon tension forces T_n in an offset position are proportional to the tendon top coordinates

Fig. 1. Double symmetric TLP.

Fig. 2. Large surge, sway and yaw.

$$T_x^n = \frac{T_n}{L}\left[\delta_x - \delta_\varphi \sin\left(\theta_n + \frac{\varphi}{2}\right)\right], \tag{5}$$

$$T_y^n = \frac{T_n}{L}\left[\delta_y + \delta_\varphi \cos\left(\theta_n + \frac{\varphi}{2}\right)\right], \tag{6}$$

$$T_z^n = \frac{T_n}{L}L_z^n. \tag{7}$$

Total tendon force acting on platform is $T = \sum_{n=1}^{N} T_n$. Its components according to (5)–(7) read

$$T_x = \sum_{n=1}^{N} T_x^n = \frac{T}{L}\delta_x, \tag{8}$$

$$T_y = \sum_{n=1}^{N} T_y^n = \frac{T}{L}\delta_y, \tag{9}$$

$$T_z = \sum_{n=1}^{N} T_z^n = \frac{T}{L}\frac{1}{N}\sum_{n=1}^{N} L_z^n. \tag{10}$$

Horizontal components T_x and T_y depend only on horizontal displacements δ_x and δ_y, respectively, since the trigonometric functions vanish from (5) and (6) upon summation owing to the platform double symmetry. However, values of L_z^n are different in case of yaw. In order to make summation of L_z^n in (10) possible let us expand L_z^n into power series. Since $\sqrt{1-\varepsilon} = 1 - \frac{1}{2}\varepsilon - \frac{1\cdot1}{2\cdot4}\varepsilon^2 - \cdots$ one can write

$$L_z = \frac{1}{N}\sum_{n=1}^{N} L_z^n = L(1 - f_1 - f_2), \tag{11}$$

where

$$f_1 = \frac{1}{2L^2}\left(\delta_x^2 + \delta_y^2 + \delta_\varphi^2\right), \quad f_2 = \frac{1}{2}f_1^2 + f_3, \tag{12}$$

$$f_3 = \frac{2}{L^4}\left[\delta_x^2\left(b^2\cos^2\frac{\varphi}{2} + a^2\sin^2\frac{\varphi}{2}\right) + \delta_y^2\left(a^2\cos^2\frac{\varphi}{2} + b^2\sin^2\frac{\varphi}{2}\right) \right. $$
$$\left. + \delta_x\delta_y(b^2 - a^2)\sin\varphi\right]\sin^2\frac{\varphi}{2}. \tag{13}$$

Functions f_1 and f_2 are the first and second order terms, respectively. Relatively simple expressions are obtained since trigonometric functions of argument θ_n with odd exponent vanish upon summation. Also, relation (1) for δ_φ, $\cos^2\theta_n = (a/r)^2$ and $\sin^2\theta_n = (b/r)^2$ are employed. In that way angles θ_n disappear from L_z. Differences $L_z^n - L_z$ cause some small platform roll and pitch.

The tendon offsets cause platform setdown $\delta^s = L - L_z$, and consequently additional buoyancy ΔU and tendon forces ΔT_n. The resulting additional tendon force can be determined from the equilibrium of the vertical forces

$$U + \Delta U = Q + \frac{1}{L}\sum_{n=1}^{N}(T_n + \Delta T_n)L_z^n, \tag{14}$$

where Q is the platform weight. The second term in (14) is written according to (10). The increased buoyancy reads

$$\Delta U = \rho g A_{WL}\delta^s, \tag{15}$$

where A_{WL} is the waterplane area. By taking floating condition $T = U - Q$ into account and substituting (15) into (14), one finds for the total additional tendon force

$$\Delta T = \frac{1}{L_z}\sum_{n=1}^{N} \Delta T_n L_z^n = \frac{1}{L_z}(T + \rho g A_{WL}L)\delta^s. \tag{16}$$

Horizontal component of the total tendon force (8) is increased, and has to be equal to the external force, $T_x = F_x$, i.e.

$$F_x = \frac{1}{L}(T + \Delta T)\delta_x = \tilde{K}_0\delta_x, \tag{17}$$

where $\tilde{K}_0$ is nonlinear secant stiffness. By substituting (16) into (17) yields

$$\tilde{K}_0 = \frac{1}{L_z}(T + \rho g A_{WL}\delta^s) = \frac{C}{L_z} - \rho g A_{WL}, \tag{18}$$

where

$$C = T + \rho g A_{WL}L. \tag{19}$$

Analogously, the sway force reads $T_y = F_y = \tilde{K}_0\delta_y$.

The yaw moment is caused by the horizontal tendon forces

$$M_z = -\sum_{n=1}^{N}(T_x^n + \Delta T_x^n)y_n + \sum_{n=1}^{N}\left(T_y^n + \Delta T_y^n\right)x_n, \tag{20}$$

where $x_n = r\cos\theta_n$ and $y_n = r\sin\theta_n$ are the tendon top coordinates, Fig. 1. By employing (5) and (6) one finds

$$M_z = \frac{r}{L}\sum_{n=1}^{N}(T_n + \Delta T_n)\left(-\delta_x\sin\theta_n + \delta_y\cos\theta_n + \delta_\varphi\cos\frac{\varphi}{2}\right). \tag{21}$$

Trigonometric functions of θ_n vanish upon summation and taking (1) for δ_φ into account one arrives at

$$M_z = \frac{r^2}{L}(T + \Delta T)\sin\varphi = \tilde{K}_0 r^2\varphi. \tag{22}$$

Since according to (17) $(T + \Delta T)/L = \tilde{K}_0$, the yaw stiffness reads

$$\tilde{K}_{66} = r^2\tilde{K}_0\frac{\sin\varphi}{\varphi}. \tag{23}$$

Function $\sin\varphi/\varphi$ represents reduction of arm of the tendon horizontal forces. For hypothetically large value $\varphi = \pi$, the arm is zero.

Fig. 3. Construction of setdown in offset plane.

2.2. Large translation and small rotation

If only the first two terms of expansion (11) for L_z are taken into account, the setdown reads

$$\delta^s = L - L_z = Lf_1 = \frac{1}{2L}\left(\delta_x^2 + \delta_y^2 + \delta_\varphi^2\right). \tag{24}$$

It can be constructed as shown in Fig. 3, where δ_h and ψ is virtual horizontal displacement and offset angle, respectively.

Furthermore, if yaw angle φ is small then according to (1) $\delta_\varphi = r\varphi$ and

$$\delta^s = \frac{1}{2L}\left(\delta_x^2 + \delta_y^2 + r^2\varphi^2\right). \tag{25}$$

In that case the yaw stiffness (23) is also simplified, $\widetilde{K}_\varphi = r^2\widetilde{K}_0$. It is obvious that stiffness in any horizontal direction is the same.

3. Stiffness based on balance of potential energy

3.1. Large translation and rotation

The following forces act on platform: U, Q, T, ΔT and ΔU. Tendon elongation ΔL_n due to tendon forces $T_n + \Delta T_n$ is very small comparing to the platform setdown and therefore is ignored. Work of the external vertical forces $U - Q = T$ is done in the way of setdown, δ^s. Buoyancy variation ΔU is internal force increasing proportionally to the setdown. Hence, one can specify the platform potential energy as

$$V = T\delta^s + \frac{1}{2}\rho g A_{WL}(\delta^s)^2. \tag{26}$$

The platform vertical coordinate L_z is defined by (11), and accordingly the setdown $\delta^s = L - L_z$ reads

$$\delta^s = L(f_1 + f_2), \tag{27}$$

where f_1 and f_2 are specified with (12) and (13), respectively. L_z can also be determined as the quadratic mean of the tendon vertical coordinates (4), i.e.

$$L_z^2 = \frac{1}{N}\sum_{n=1}^{N}(L_z^n)^2. \tag{28}$$

Since the trigonometric functions of angles θ_n in $(L_z^n)^2$ vanish upon summation, yields

$$L_z^2 = L^2(1 - 2f_1). \tag{29}$$

On the other side, relation $\delta^s = L - L_z$ gives

$$(\delta^s)^2 = L^2 - 2LL_z + L_z^2. \tag{30}$$

By substituting (11) and (29) into (30) one arrives at

$$(\delta^s)^2 = 2L^2 f_2. \tag{31}$$

Finally, by employing (27) and (31), Eq. (26) can be presented in the form

$$V = TLf_1 + CLf_2, \tag{32}$$

where function f_2 of the second order is transferred from the first term to the second one.

Since function f_2 consists of two terms, Eq. (12), yields

$$V = TLf_1 + \frac{1}{2}CLf_1^2 + CLf_3, \tag{33}$$

Restoring forces are obtained as derivatives of the potential energy per particular displacement. Hence, for the secant stiffness of surge, sway and yaw one can write

$$\widetilde{K}_{11} = \frac{L}{\delta_x}\left(T\frac{\partial f_1}{\partial \delta_x} + C\frac{\partial f_2}{\partial \delta_x}\right), \tag{34}$$

$$\widetilde{K}_{22} = \frac{L}{\delta_y}\left(T\frac{\partial f_1}{\partial \delta_y} + C\frac{\partial f_2}{\partial \delta_y}\right), \tag{35}$$

$$\widetilde{K}_{66} = \frac{L}{\varphi}\left(T\frac{\partial f_1}{\partial \varphi} + C\frac{\partial f_2}{\partial \varphi}\right). \tag{36}$$

Derivatives of functions f_1 and f_2, Eqs. (12) and (13), are the following:

$$\frac{\partial f_1}{\partial \delta_x} = \frac{\delta_x}{L^2}, \frac{\partial f_1}{\partial \delta_y} = \frac{\delta_y}{L^2}, \frac{\partial f_1}{\partial \varphi} = \frac{r^2}{L^2}\sin\varphi, \tag{37}$$

$$\frac{\partial f_2}{\partial \delta_x} = \frac{1}{L^2}f_1\delta_x + \frac{4}{L^4}f_3\delta_x\sin^2\frac{\varphi}{2}, \tag{38}$$

$$\frac{\partial f_2}{\partial \delta_y} = \frac{1}{L^2}f_1\delta_y + \frac{4}{L^4}f_4\delta_y\sin^2\frac{\varphi}{2}, \tag{39}$$

$$\frac{\partial f_2}{\partial \varphi} = \frac{r^2}{L^2}f_1\sin\varphi + \frac{1}{L^4}\left[f_4\delta_x^2 + f_5\delta_y^2 + (b^2 - a^2)\delta_x\delta_y\sin\varphi\right]\sin\varphi$$
$$+ \frac{b^2 - a^2}{L^4}\left[\left(\delta_y^2 - \delta_x^2\right)\sin\varphi + 2\delta_x\delta_y\cos\varphi\right]\sin^2\frac{\varphi}{2}, \tag{40}$$

where f_1 is represented with (18) and

$$f_4 = b^2\cos^2\frac{\varphi}{2} + a^2\sin^2\frac{\varphi}{2}, \tag{41}$$

$$f_5 = a^2\cos^2\frac{\varphi}{2} + b^2\sin^2\frac{\varphi}{2}. \tag{42}$$

3.2. Large translation and small rotation

If yaw angle is small $\sin\varphi \approx \varphi$, $\cos^2\frac{\varphi}{2} \approx 1$ and $\sin^2\frac{\varphi}{2} \approx 0$, the stiffness elements, Eqs. (34)–(36), take quite simple form

$$\widetilde{K}_{11} = \widetilde{K}_0 + \frac{C}{L^3}b^2\varphi^2, \tag{43}$$

$$\widetilde{K}_{22} = \widetilde{K}_0 + \frac{C}{L^3}a^2\varphi^2, \tag{44}$$

$$\widetilde{K}_{66} = r^2\widetilde{K}_0 + \frac{C}{L^3}\left[b^2\delta_x^2 + a^2\delta_y^2 + (b^2 - a^2)\delta_x\delta_y\right], \tag{45}$$

where $\widetilde{K}_0$ is specified with Eq. (34). Last term in (53) in case of a square platform is zero, while for a rectangular one its value depends on the platform aspect ratio. If that term is ignored due to small value, elements $\widetilde{K}_{ii}$, $i = 1, 2, 6$, are identical to those presented in [10]. They are derived directly for small yaw angle and utilizing the energy approach based on the assumption that each platform quarter moves separately together with the corresponding tendon.

4. Stiffness based on root means square of tendon forces

4.1. Large translation and rotation

In spite of the fact that stiffness elements shown in the previous sections are consistently derived based on equilibrium of forces and energy balance, different formulas are obtained. The reason for that is use of the algebraic and quadratic mean of the vertical tendon forces, expressed with coordinates L_z^n, Eq. (10), in the former and latter case, respectively. Consequence of natural application of the algebraic mean on potential energy is investigated in Appendix.

In addition it is interesting to apply the quadratic mean for vertical tendon forces in the force equilibrium approach. One can start with rigorous expression for $\widetilde{K}_0$, Eq. (18). Since $L_z = L - \delta^s$ and by employing relation $(1 - \varepsilon)^{-1} \approx 1 + \varepsilon$, yields

Table 1
Main particulars of the ISSC TLP.

Parameters	Symbol	Value
Column (tendon) spacing	$2a = 2b$	86.25 m
Column diameter	D_C	16.87 m
Pontoon width	w	7.50 m
Pontoon height	d	10.50 m
Draft	$-z_T$	35.00 m
Waterplane area	A_{wl}	894 m^2
Displacement	U	5.346×10^5 kN
Weight	Q	3.973×10^5 kN
Total tendon pretension	T	1.373×10^5 kN
Longitudinal metacentric height	$\overline{M_L G}$	6.0 m
Transverse metacentric height	$\overline{M_T G}$	6.0 m
Platform mass	m	40.5×10^3 t
Roll mass moment of inertia	J_x^G	82.37×10^6 t m^2
Pitch mass moment of inertia	J_y^G	82.37×10^6 t m^2
Yaw mass moment of inertia	J_z^G	98.07×10^6 t m^2
Vertical position of COG above keel	$\overline{PG}$	38.0 m
Vertical position of COB above keel	$\overline{PB}$	22.3 m
Length of mooring tendons	L	415.0 m
Tendon cross-section area	A	1.6 m^2
Vertical stiffness of combined tendons	$\frac{EA}{L}$	0.813×10^6 kN/m
Roll and pitch effective stiffness	$\frac{EI_x}{L}, \frac{EI_y}{L}$	1.501×10^9 kNm/rad
Young's modulus	E	2.1×10^8 kN/m^2

$$\widetilde{K}_0 = \frac{T}{L} + \frac{C}{L^2} \delta^s. \tag{46}$$

For setdown δ^s quadratic mean (31), i.e. root mean square, can be used that arrives at

$$\widetilde{K}_{RMS} = \frac{T}{L} + \frac{C}{L^2} \delta_{RMS}^s, \tag{47}$$

where

$$\delta_{RMS}^s = L\sqrt{2f_2}. \tag{48}$$

By employing the second of Eqs. (12) the stiffness is presented in the final form

$$\widetilde{K}_{RMS} = \frac{T}{L} + \frac{C}{L} \sqrt{f_1^2 + 2f_3}. \tag{49}$$

4.2. Large translation and small rotation

If yaw angle is small one finds from Eqs. (12) and (13)

$$f_1 = \frac{1}{2L^2}\left(\delta_x^2 + \delta_y^2 + r^2\varphi^2\right), \tag{50}$$

$$f_3 = \frac{1}{2L^4}\left(b^2\delta_x^2 + a^2\delta_y^2\right)\varphi^2. \tag{51}$$

In that case $2f_3 \ll f_1^2$ and relation $\sqrt{1+\varepsilon} \approx 1+\frac{\varepsilon}{2}$ can be applied. By taking into account $\delta^s = L f_1$ stiffness (49) can be presented in the form

$$\widetilde{K}_{RMS} = \widetilde{K}_0 + \frac{C}{2L^4\delta^s}\left(b^2\delta_x^2 + a^2\delta_y^2\right)\varphi^2. \tag{52}$$

The stiffness is the same in any direction, while that obtained by the energy approach is different, Eqs. (43)–(45). Actually, the constitutive quantities of (52) are spread into Eqs. (43)–(45) in a refined energetic way. Yaw influences translations and vice versa.

5. Comparison analysis of different stiffness formulations

5.1. Uncoupled static analysis

Influence of six restoring stiffness formulations presented in Sections 2–4, on uncoupled static platform response, i.e. ignoring tendon influence, is analysed in the case of well known ISSC TLP, which is often used in the relevant literature as a benchmark [12]. The platform main particulars are listed in Table 1, where tension leg stiffness and mass parameters are related to the center of gravity.

Large surge and yaw displacements are given in order to magnify their coupling: $\delta_x = 0.1L = 41.5$ m and $\varphi = 45° = 0.78537$ rad. The surge force $F_x = \widetilde{K}_0\delta_x$ and yaw moment $M_z = r^2\widetilde{K}_0\varphi$, are calculated by employing formula (34) for $\widetilde{K}_0$. The partial setdown for surge and yaw are determined according to (25):

$$\delta_F^s = \frac{1}{2L}\delta_x^2 = 2.075 \text{ m},$$

$$\delta_M^s = \frac{r^2}{2L}\varphi^2 = 2.748 \text{ m}.$$

That leads to $F_x = 1.563 \times 10^4$ kN and $M_z = 1.136 \times 10^6$ kN m.

Furthermore, force F_x and M_z are imposed to the platform separately and than together in order to analyse interaction between surge and yaw. The obtained results for uncoupled and coupled case and six stiffness formulations, determined iteratively, are listed in Table 2. All formulations in case of F_x give the same value for δ_x and δ^s, respectively. Moment M_z causes almost the same displacements φ and δ^s, for force equilibrium and energy balance. Differences of ca. 20% are caused by yaw treatment as a small or large quantity. Common action of F_x and M_z results with different values of all displacements, δ_x, φ, δ^s, for considered six cases, i.e. three different approaches and two yaw treatments.

In order to evaluate which of the above results are more realistic, the same nonlinear problem is solved by the finite element method by using program LS DYNA [13]. A quite simple FEM model is constructed as shown in Fig. 4. The platform is modeled as a thick plate of thickness $t = 1$ m and tendons by one finite element. Force F_x is lumped in the plate corners, while moment M_z is distrib-

Table 2
Platform displacements.

Case no.	Approach	Averaging of tendon forces	Yaw treatment	Loading condition Ref.	$F_x = 1.563 \times 10^4$ kN		$M_z = 1.136 \times 10^6$ kN m		$F_x \& M_z$		
					δ_x (m)	δ^s (m)	φ (°)	δ^s (m)	δ_x (m)	φ (°)	δ^s (m)
1	Force equilibrium	Arithmetic	Small	[9] Section 2.2	41.5	2.075	45	2.748	37.174	41.87	4.044
2	Force equilibrium	Arithmetic	Large	Section 2.1	41.5	2.075	50	3.392	36.604	46.01	4.336
3	Force equilibrium	RMS	Small	Section 4.2	41.5	2.075	45	2.748	36.110	40.67	3.815
4	Force equilibrium	RMS	Large	Section 4.1	41.5	2.075	50	3.392	35.596	44.40	4.071
5	Energy balance	Quadratic	Small	[10] Section 3.2	41.5	2.075	45	2.748	34.204	39.98	3.579
6	Energy balance	Quadratic	Large	Section 3.1	41.5	2.075	50	3.182	33.330	43.79	3.817
7	FEM			LS DYNA	41.25	2.055	49.1	3.088	33.343	42.95	3.746
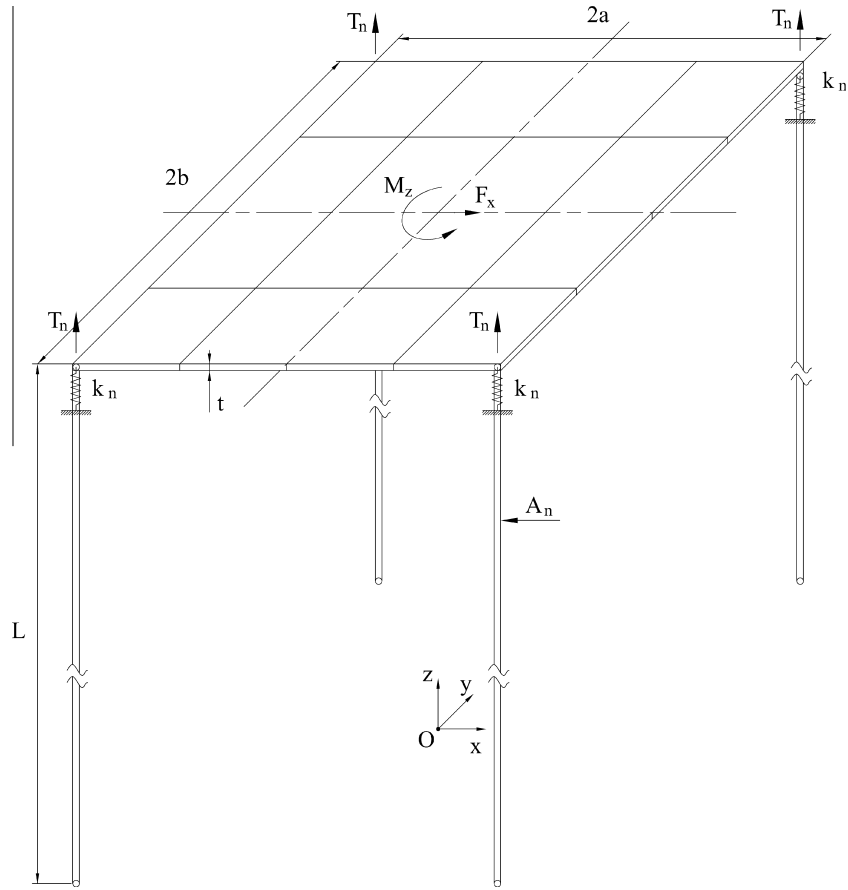
Fig. 4. TLP FEM model.
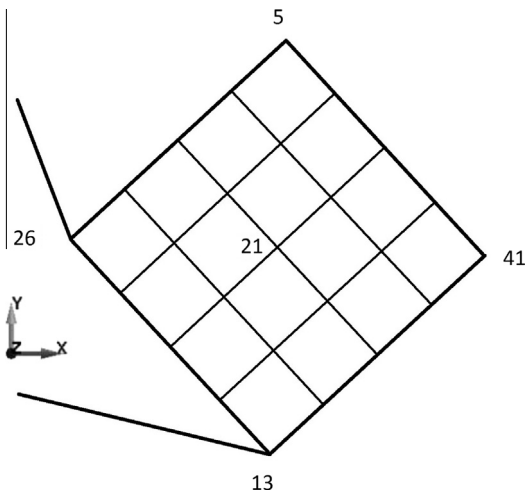
Fig. 5. Bird's view of platform in offset position.
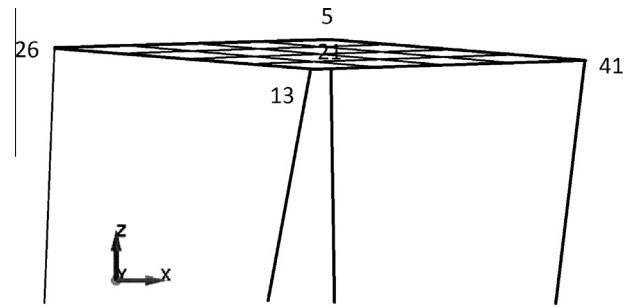
Fig. 6. Lateral view of platform in offset position.

to avoid inertia influence. First force F_x is imposed and then moment M_z so that their particular influence on response can be noticed. The bird's view of the platform in the equilibrated translated and rotated position is shown in Fig. 5. Figs. 6 and 7 show zoomed lateral and front view, where platform small pitch and roll can be noticed.

The time history of the platform longitudinal, transversal and vertical displacements is shown in Figs. 8–10, respectively. During F_x action displacements of all platform corners are the same. By activating M_z spreading of displacements due to rotation is noticeable. Displacement δ_x is slightly reduced, while setdown δ^s is considerably increased.

The FEM results for all three loading conditions are added in Table 2. Response due to F_x is slightly smaller than the analytical values. In case of M_z action numerical results are also somewhat lower than analytical ones for energy balance approach and yaw treat-

uted in all 25 nodes. The hydrostatic springs in the plate corners take value $k_n = \frac{1}{4}\rho g A_{WL} = 2192$ kN/m. Value of the Young's modulus is considerably increased ($E^* = 10^3 E$) in order to constrain initial tendon strain due to imposed tendon pretension forces T_n, Fig. 4.

Numerical calculation is performed separately for particular loads F_x and M_z, and then for their common action. Due to geometric nonlinearity caused by the large displacements the static problem is solved as a dynamic one in the time domain by the step-by-step integration method and slowly increasing load values in order

Fig. 7. Front view of platform in offset position.
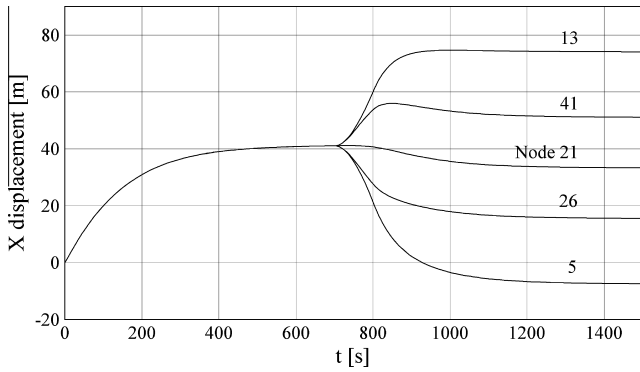
Fig. 8. Time history of platform longitudinal displacement.
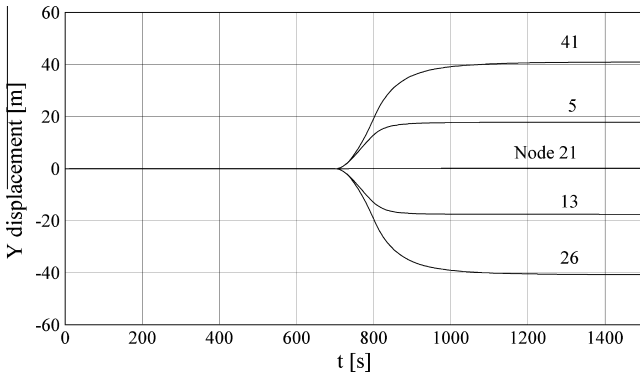
Fig. 9. Time history of platform transverse displacement.
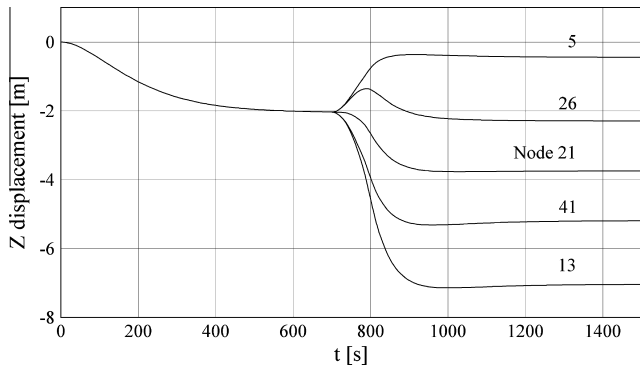
Fig. 10. Time history of platform setdown.
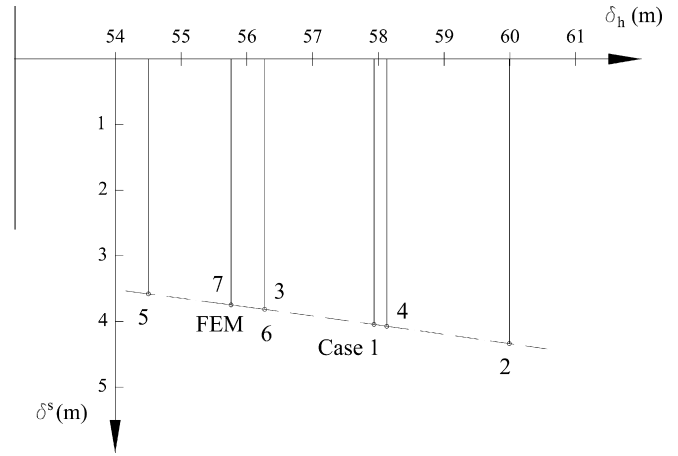
Fig. 11. Setdown versus virtual horizontal displacement.
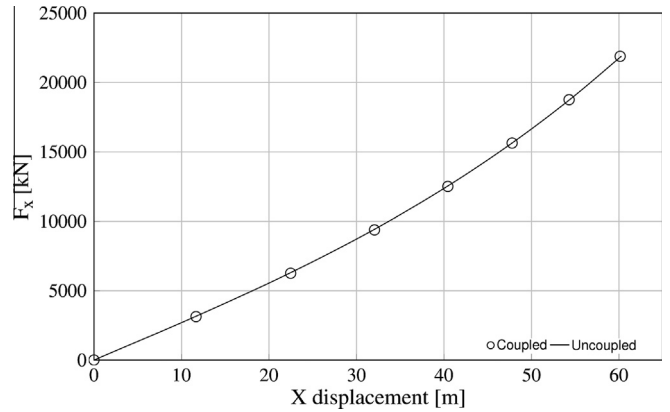
Fig. 12. Horizontal restoring force versus horizontal displacement.

ment as a large value. Since the analytical solutions for particular load are rigorous, they can be used for validation of the FEM results.

For simultaneous action of F_x and M_z the analytical results are nearly equal to the numerical ones. However, the latter are more accurate and therefore are used as referent values. Values of setdown in cases 3 and 6 are closer to the FEM ones, than those obtained for the other four cases. However, in case 6 better agreement for surge and yaw is obtained. Spreading of setdown δ^s as function of virtual horizontal displacement, $\delta_h = \sqrt{2L\delta^s}$, which comprises both surge, δ_x, and yaw, δ_φ, Eq. (24), is shown in Fig. 11. The figure represents zoom of the complete diagram constructed in accordance with Fig. 3.

5.2. Coupled static analysis

The ISSC TLP is exposed to action of static surge force F_x, imposed at the pole level P, Fig. 1, by gradually increasing its magnitude. In analytical uncoupled analysis one half of the tendon weight is added to the platform bottom and another half to the sea bottom.

The same task is analysed as coupled platform and tendon problem by the finite element method, [14] and [15]. The platform is represented by one rigid plate element, while each tendon is modeled by four beam finite elements with realistic stiffness and distributed weight.
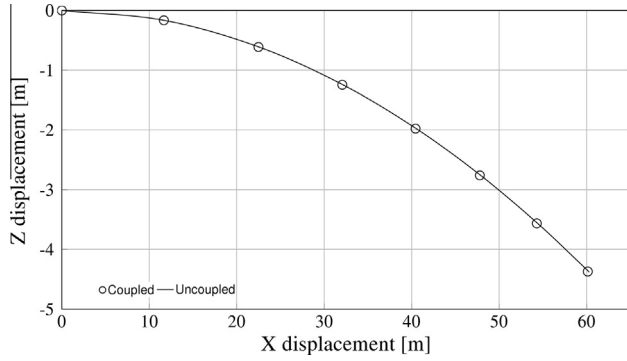
Fig. 13. Vertical displacement versus horizontal displacement.

Table 3
Comparison of coupled (FEM) and uncoupled (analytical) TLP static analysis.

F_x (kN)	Coupled		Uncoupled	
	X (m)	Z (m)	X (m)	Z (m)
0	0.000	0.000	0.000	0.000
3126	11.667	−0.165	11.559	−0.161
6252	22.482	−0.613	22.327	−0.601
9378	32.066	−1.245	31.926	−1.228
12,504	40.444	−1.979	40.355	−1.962
15,630	47.793	−2.763	47.770	−2.749
18,756	54.304	−3.565	54.350	−3.559
21,882	60.135	−4.372	60.251	−4.374

The obtained results are shown in Figs. 12 and 13. The former represents surge as function of imposed force F_x, and latter shows vertical displacement as function of surge. Difference between analytical uncoupled and FEM coupled analysis is very small as can be noticed in Table 3. In uncoupled analysis vertical displacement is pure setdown, while in coupled analysis there is small release due to tendon elasticity. Since results of uncoupled and coupled analysis are very close, one can conclude that the former is reliable enough for the static analysis.

6. Conclusion

Nonlinear restoring stiffness plays very important role in TLPs dynamic behavior. The traditionally used stiffness matrix manifests shortcomings [7,8], while there is doubt concerning consistency of the recently derived matrix [10]. Therefore a detailed analysis of the problem is undertaken. Both the force equilibrium approach, with algebraic mean and RMS of tendon forces, and potential energy approach with quadratic mean are used and new stiffness matrices, treating yaw as a small and large displacement, are derived. Comparison of numerical results determined for ISSC TLP with those of FEM analysis shows that the stiffness matrix formulation based on energy approach for large yaw is the most reliable.

The derived secant stiffness matrix for horizontal motions has to be completed with terms for vertical motions, i.e. heave, pitch and roll. Such matrix is diagonal since it is established with respect to the pole P, Fig. 1, while the accompanying mass matrix is not diagonal. Setdown, as a slave d.o.f. of the master horizontal displacements, induces vertical inertia force, which has to be incorporated in the mass matrix. However, it is easier to add setdown to heave forming in such a way complete vertical motion. The stiffness matrix is accordingly transformed; it becomes asymmetric [9]. In order to perform dynamic analysis in ordinary way with respect to the center of gravity, both matrices have to be transformed

from the tendon natural coordinate system to the global system with origin in the center of gravity.

Some software operate with nonlinear restoring forces and some with their increments, i.e. secant and tangent stiffness matrix, respectively. Both matrices can be easily incorporated in the existing computer codes. In that way applicability and accuracy of uncoupled model is extended and increased, respectively. That might be interesting for improvement of the required uncoupled time domain model in the Classification Rules for design and construction of TLPs, [16].

Appendix A. Potential energy based on equilibrated forces

After the nonlinear stiffness for large translation and small rotation and algebraic mean of tendon forces based on equilibrium of internal and external forces is established, it is interesting to formulate potential energy of the considered elastic system. The external forces are specified in simple form

$$F_x = \widetilde{K}_0 \delta_x, \quad F_y = \widetilde{K}_0 \delta_y, \quad M_z = r^2 \widetilde{K}_0 \varphi, \tag{A1}$$

where $\widetilde{K}_0$ is common stiffness, Eq. (18). Since $L_z = L - \delta^s$, stiffness, Eq. (18) can be expressed as function of setdown

$$\widetilde{K}_0 = \frac{C}{L - \delta^s} - \rho g A_{WL}. \tag{A2}$$

Work of the horizontal forces is

$$V = \int F_x \, d\delta_x + \int F_y \, d\delta_y + \int M_z \, d\varphi \tag{A3}$$

and by substituting (A1) into (A3) yields

$$V = \int \widetilde{K}_0 (\delta_x \, d\delta_x + \delta_y \, d\delta_y + r^2 \varphi \, d\varphi). \tag{A4}$$

Expression in the brackets, according to (25), represents the total differential of setdown, i.e. $(\ldots) = L \, d\delta^s$. Hence, by substituting (18) into (A4) one finds

$$V = L \int \left(\frac{C}{L - \delta^s} - \rho g A_{WL} \right) d(\delta^s)$$
$$= -LC \ln \left(1 - \frac{\delta^s}{L} \right) - \rho g A_{WL} L \delta^s. \tag{A5}$$

The logarithmic function can be expanded into the power series

$$\ln \left(1 - \frac{\delta^s}{L} \right) = -\sum_{k=1}^{\infty} \frac{1}{k} \left(\frac{\delta^s}{L} \right)^k, \tag{A6}$$

that leads to

$$V = T\delta^s + \frac{C}{2L} (\delta^s)^2 + LC \sum_{k=3}^{\infty} \frac{1}{k} \left(\frac{\delta^s}{L} \right)^k, \tag{A7}$$

where the first two term of the series are expressed explicitly. Quantities C and δ^s are specified by Eqs. (19) and (25), respectively. According to (12) $\delta^s = L f_1$ and the potential energy can be presented in the following form

$$V = TLf_1 + \frac{1}{2} CLf_1^2 + LC \sum_{k=3}^{\infty} \frac{1}{k} f_1^k. \tag{A8}$$

By comparing (A8) with (33) it is obvious that the first two terms are identical. The third term in (33) is of the same order of magni-

tude as the second one, and cannot be compensated with the third term in (A8), since it is a small quantity of higher order.

Formulation of potential energy (A8) leads to the stiffness

$$\widetilde{K}_0 \approx \frac{T}{L} + \frac{C}{L^2}\delta^s, \tag{A9}$$

which is common for any direction. The first and the second term in (A9) represent linear and nonlinear stiffness, respectively, [9].

References

[1] Chakrabarti S. Handbook of offshore engineering. Elsevier Science; 2005.
[2] Planning, designing and constructing tension leg platforms. API recommended practice 2T, 3rd ed. American Petroleum Institute; 2010.
[3] Adrezin R, Bar-Avi P, Benaroya H. Dynamic response of compliant offshore structures – review. J Aerosp Eng 1996;9(4):114–31.
[4] Faltinsen OM, Demirbilek Z. Hydrodynamic analysis of TLPs. In: Demirbilek Z, editor. Tension leg platform: a state-of-the-art review. ASCE; 1989. p. 36–63.
[5] DNV – OS – C105 Structural design of TLP (LRFD method). Det Norske Veritas; 2008.
[6] Morgan J, Malaeb D. Dynamic analysis of tension leg platforms. In: Proceedings of the second international offshore mechanics and arctic engineering symposium; 1983. p. 31–7.
[7] Jain AK, Nonlinear coupled response of offshore tension leg platform to regular wave forces. Ocean Eng 1997;24(7):577–93.
[8] Chandrasekaran S, Jain AK. Dynamic behavior of square and triangular offshore tension leg platforms under regular wave load. Ocean Eng 2002;29(3):279–313.
[9] Senjanović I, Tomić M, Hadžić N. Formulation of consistent nonlinear restoring stiffness for dynamic analysis of tension leg platform and its influence on response. Marine Struct 2013;30(1):1–32.
[10] Low YM. Frequency domain analysis of a tension leg platform with statistical linearization of the tendon restoring forces. Marine Struct 2009;22(3):480–503.
[11] Murray J, Yang CK, Yang W, Krishnaswamy P, Zou J. An extended tension leg platform design for Post-Katrina Gulf of Mexico. In: The proceedings of the nineteenth international offshore and polar engineering conference (ISOPE), vol. 1; 2009. p. 120–7.
[12] Taylor RE, Jefferys ER. Variability of hydrodynamic load predictions for a tension leg platform. Ocean Eng 1986;13(5):449–90.
[13] LS DYNA theory manual. Livermore Software Technology Corporation; 2006.
[14] Garrett DL. Dynamic analysis of slender rods. J Energy Resour Technol 1982;104(4):302–6.
[15] Ćatipović I, Čorić V, Vukčević V. Dynamics of FPSO with polyester mooring lines. In; Proceedings of the twenty-second international offshore and polar engineering conference; 2012. p. 996–1003.
[16] Rules for the classification of tension leg platforms (TLP). Bureau Veritas; 2012.